Performance of a New Design Based on Substrate-Integrated Waveguide Slotted Antenna Arrays for Dual-Band Applications (*Ku / K*)

Abes Turkiya, Nouri Keltouma, Bouazza Boubakar Seddik, and Becharef Kada

***Abstract*—This paper introduces and discusses the study of a new concept for SIW array antenna development. This conducted development is based on three designs, two of them related to 1x2 arrays fed by SIW line, combined with SIW inset line, and the last designed for 2X2 array antenna feed by SIW inset line. All these structures are designed to give dual-band at (Ku - K) bands with enhanced gain and bandwidth. The new 2x2 array antenna has a high gain, and it consists of four SIW cavities staggered patches with a 90° phase shift, which are fed using microstrip line shielded by SIW vias. The designs were conducted using full-wave simulator ANSYS HFSS - the frequency domain solver. The 2x2 array antenna gives a return loss about (-20 dB), a high gain of 9.05 dB, and two bandwidth equals 210 MHz and 1310 MHz respectively at both of the operating bands. To validate the simulated results the simulation was conducted again using the time-domain solver of the CST Microwave Studio (MWS) full-wave simulator. Simulation results obtained from the two software having different solvers were in good agreement in the results.**

***Index terms*—Antenna Arrays, SIW technology, slot, gain, and (K_U *-K)* band.**

I. INTRODUCTION

In a communication system, the antennas must be adapted to fulfill the requirements of the new applications. They have to match the constraints on the operating frequency bands and be easy to integrate by ports of other circuits [1]. New telecommunication systems have shown the inadequacy of conventional antennas performance, and they need a new type of multi-band antennas, the principle of having a single antenna that offers more than operating frequency at multi bands [1].

On the other hand, this type of antennas sufferers from limited performance related to the gain and bandwidth. High gain antennas have many applications in wireless communication systems as they produce focused radiating beams and narrow beamwidth, which allows for more precise direction of the signal. On the other hand, these antennas usually have large size and weight, which lead to high shipping expenses and heavy manpower expenditure on equipment installation and adjustment [1, 2]. These considerations drive us to develop a new with a high-gain and wideband planar antenna as an alternative for these non-planar antennas [3].

When the emerges application requires more restricted specifications that include specific electromagnetic performance, whether, related to the form of a radiation lobe, high gain or to the bandwidth, it is necessary to use array antennas to meet with these requirements [4]. Microstrip fed array antennas have been extensively used in microwave applications [3]. However, the feeding efficiency of μ-strip lines drops significantly due to the serious losses at bends and discontinuities when the operating frequency goes up to the millimeter-wave bands. A low-loss, high-efficiency, planar feeding network is required [4, 5, 6].

The Substrate-integrated waveguide (SIW) technology combines the superior characteristics of the planar transmission line and the non-planar waveguide and therefore can provide more expectations to have high-performance millimeter-wave circuits at low manufacturing costs [7,8]. There are radiation leakage and coupling which can be neglectable, even at SIW bends and discontinuities. Therefore, it is a good solution for millimeter-wave feeding network applications [1, 9, 10]. The SIW technology was proposed as an alternative technique to facilitate the low-cost implementation of waveguide-like components utilizing the standard PCB technology fabrication technics [11]. under principal conditions, like using via holes properly spaced at about λg/20, to ensure that the shield of the conventional waveguide sidewalls could be realized using the vias rows [12]. This technology was utilized in [3, 4] to achieve a low cost, relatively low loss feed array antennas [13, 14]. In a traditional SIW, electromagnetic waves are confined to a dielectric body enclosed by the upper and lower metal walls of the substrate and by lateral metallic cylindrical holes (see Fig.1).

In our work, electromagnetic fields move in a vacuum and are confined by lower and lateral metal walls. This structure is constructed using cylindrical holes integrated into a planer

Manuscript received December 14, 2019; revised April 05, 2020. Date of publication June 5, 2020. Date of current version June 5, 2020.

Authors are with the Faculty of Technology, University Dr. Moulay Tahar Saida, Algeria (e-mails: t.abes@hotmail.fr, keltoum_nouri@yahoo.fr, bsbouazza@yahoo.fr, becharef_kada@yahoo.fr).

Digital Object Identifier (DOI): 10.24138/jcomss.v16i2.972

substrate. by this method, the sidewalls of the SIW cavities are created. this process is provided in detail at Sections II and III.

Also, the feeding networks of the proposed arrays antenna are based on SIW technology in order to minimize transmission and radiation losses of the feeding part in comparison with µ-strip line feeding. The array antenna design is carried out to operate on both of (Ku - K) bands applications. These bands are allocated to radar and amateur satellite applications [15, 16]. Two of 1x2 and 2x2 array antennas based on Integrated Substrate Waveguide (SIW), the principle of insertion of the metallic vias into the substrate are proposed in this paper. For the sake of validation of the obtained results, the designed antennas were simulated using the HFFSS simulator after that the simulation was conducted again using CST MWS to ensure the simulation accuracy.

The document is organized as follows: section II deals with the design of the single-band antenna and brief analysis of the performance of the single-element SIW sawtooth patch antenna; section III presents the simulation results of the single-item antenna design. Section IV presents the implementation of the 1x2 antenna network and exhibit the obtained results in Section V. Finally, the results of the design of the SIW 1x2 and 2x2 antenna arrays are validated by the CST Simulator running the time domain solver and compared to the frequency field results of the ANSYS High Frequency Structure Simulator (HFSS).

II. Basic Antenna Structure

A. New Circular SIW Resonant Cavity

In this work, a new circular resonant cavity is proposed. This cavity was established by SIW technology, the sidewalls of the waveguide being replaced by rows of metalized holes, the bottom represents the ground plane. While the upper face at the level of the holes of the circular SIW cavity is not metalized.

Fig. 1 illustrates the topology of this cavity. The input and output microstrip lines are used to excite cavity mode and to connect with other devices, with a vector network analyzer (VNA) to measure of dispersion parameters. Fig. 1 illustrates the topology of this cavity.

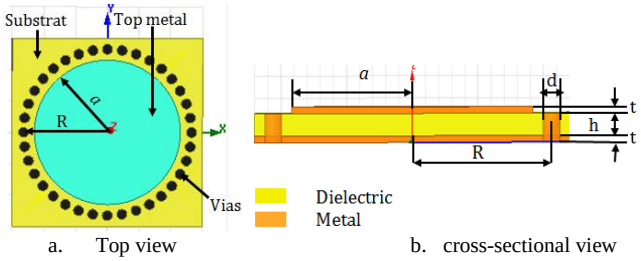

a. Top view b. cross-sectional view

Fig. 1. The topology of the SIW circular cavity without upper metallization

The design of the Circular SIW (CSIW) cavity is built using the Rogers RT/duroid TM 5880 substrate, with a thickness of 0.508 mm, the dielectric permittivity of 2.2, and loss tangent of 0.0009. The electromagnetic field distribution of the fundamental mode TM_{010} of the cylindrical resonant cavity with a circular section is given by the following figure.

The maximum electric fields are concentrated inside the cavity limited by the metalized via and symmetric along the AB plane. The simulated results of *S-parameter* for the proposed circular cavity are illustrated in Fig. 3. It operates in the range frequency from 10 to 22 GHz, giving a resonant peak at 13.83 GHz. These results are obtained through *HFSS simulation* software. It can be seen that the bandwidth of the transition covers almost the entire Ku- and K-bands. A good return loss characteristic is obtained at the operating frequency which appears approximately better than (-47.77 dB).

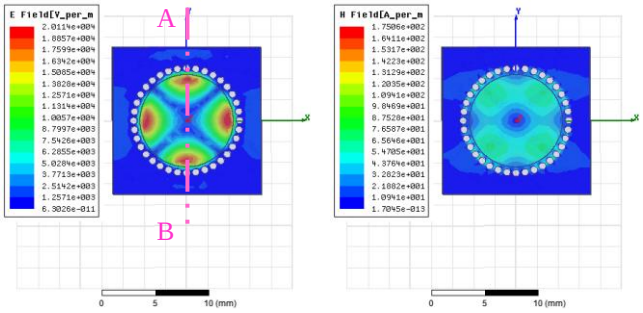

a. E field distribution b. H field distribution

Fig. 2. Electromagnetic field distributions of a circular cavity at 20 GHz

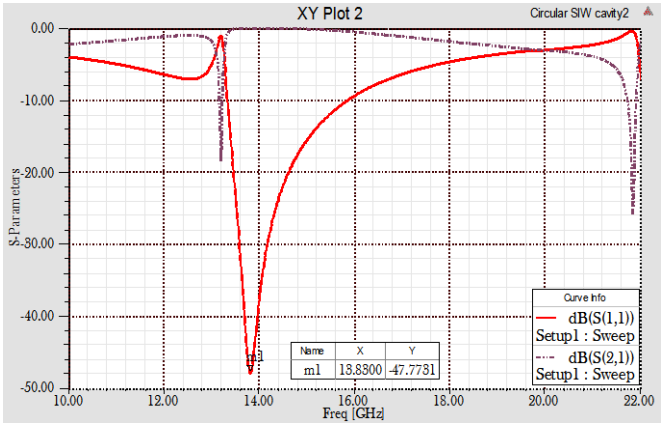

Fig. 3. Simulated scattering parameters of the resonant cavity

This proposed topology has excellent potential for high-frequency applications; it is used for the *following designs* of circular antennas in the *Ku* and *K* bands.

B. SIW Single Element Sawtooth Patch Antenna

The first step in designing an antenna is to select the proper substrate. We must choose the proper which substrate depends on its availability, application, cost and losses and the use of SIW technology, it is aimed to design a low cost, compact and high gain sawtooth patch antenna based on technology SIW. To achieve these goals, we have kept the dielectric substrate (Rogers RT/duroid TM 5880) of the SIW cavity for our topologies of sawtooth patch antenna for *Ku/K* band applications.

In single structures shown in Fig. 4 below, two slots antennas are compared, the first is with a circular slot and the second is with the octagonal slot. The dimensions of the proposed antenna are tabulated in Table I.

This new design consists of changing the topology of the SIW antenna, by removing the upper metallic layer at the level of the "vias". The linear array of metal vias is connecting with metallic surfaces only at the bottom. Therefore, new antennas and transitions are designed with these new topologies in Fig. 4.

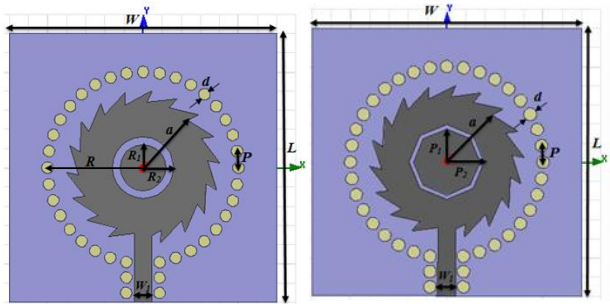

Fig.4. Topologies of the Single Element Microstrip Sawtooth Antenna with SIW

TABLE I
PROPOSED ANTENNAS PARAMETERS

parameters	W	L	d	P	W_1	R_1	R_2
Values (mm)	14	14	0.6	1.4	0.9	1.2	1.6

The resonance frequencies of the circular SIW cavity are calculated by the equations (1) to (5) as given below respectively[17].

$$f_r^{TM}{}_{010} = \frac{c}{2\pi\sqrt{\mu_r \varepsilon_r}}\sqrt{\left(\frac{2.4049}{R_{eq}}\right)^2} \quad (1)$$

where: R_{eq} is defined as [15]:

$$\mathrm{Re}\,q = R\left[1-\alpha_1\left(\frac{p}{R}\right)^2\right]-\alpha_0 \quad (2)$$

To minimize the leakage between metallic via holes, the pitch distance between circular metallic via (p) needs to be reduced and the diameter of circular metallic via holes (d) needs to be considered. To determine the diameter (d) and pitch (p), we have to commit to the criteria stated by [17] and illustrated on the expressions (3), and (4)

$$d\langle P\langle 2d \quad (3)$$

$$d\langle 4R/25 \quad (4)$$

where*:*

c: is the speed of light,

d: is the diameter of the vias,

P*:* the space of the center to center of the vias,

μ_r : Permeability of the dielectric,

ε_r : Relative dielectric permittivity.

The values of coefficients α_0 and α_1 are determined in Table II.

TABLE II
THE α_0, α_1 COEFFICIENTS IN DESIGN EQUATION

R (mm)	α_0	α_1
$1.5\langle R\langle 4.1$	0.0851	0.3208
$4.2\langle R\langle 9$	0.2240	0.8407

and:

$$f_r^{TM}{}_{110} = \frac{C}{2\pi\sqrt{\mu_r \varepsilon_r}}\sqrt{\left(\frac{1.8412}{a}\right)^2} \quad (5)$$

The radius of the patch in both designs is (a= *4mm*) is the optimal radius of a circular patch operating in the Ku/K band application. In the single element structure shown in Figure 4 with a circular slot the simulated reflection coefficient is obtained below (-10dB) and the gain of the microstrip antenna integrated with SIW is *4.82 dB.*

The bandwidths achieved by the SIW sawtooth antenna are in detail in Table IV. The 2D plots of the far-field radiation pattern, gain and electric field distributions of the designed antenna are shown in Fig. 6 (a, b and c) respectively.

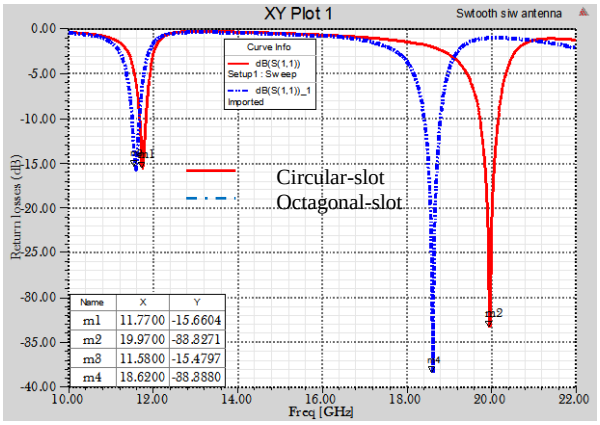

Fig. 5. S_{11} plot of the designed SIW circular sawtooth patch antenna

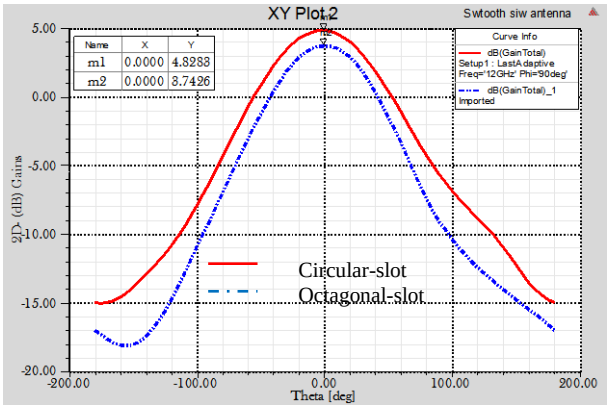

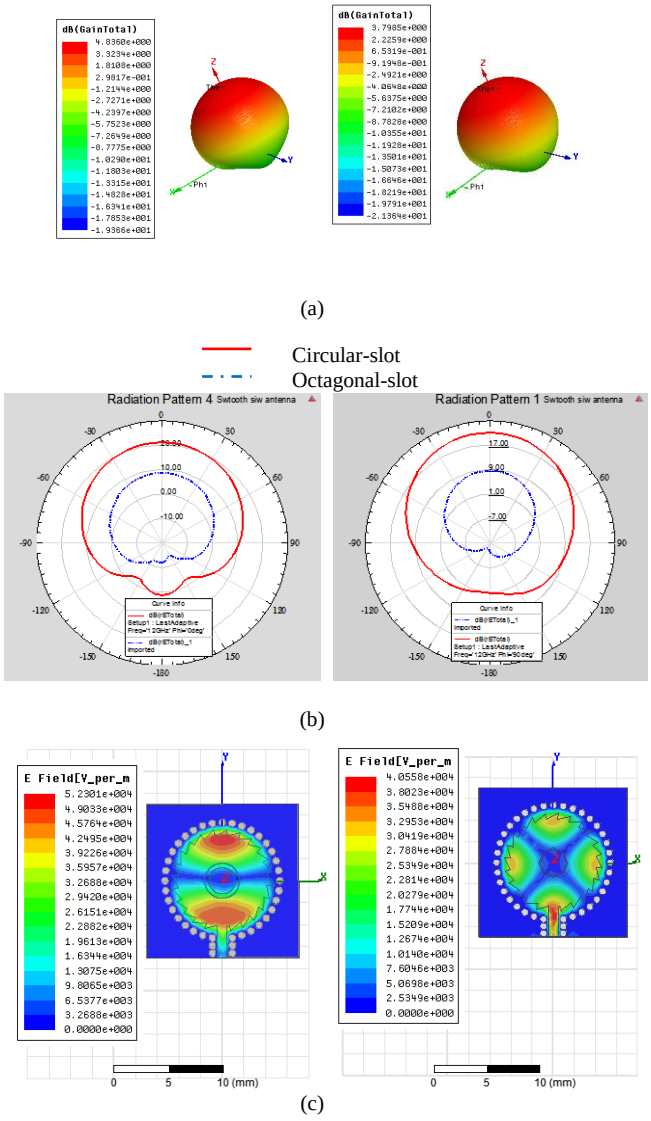

Fig. 6. Electrical characteristics of a SIW singles antennas: (a) 2D and 3D Gains, (b) Radiation patterns, (c) E-fields

After obtaining the simulation results of a single element, we observe that the insertion of the SIW holes in the substrate enhances the performance of our antenna related to the gain and bandwidth and our goal is achieved, so we went to study two new 1x2 arrays antennas with different forms of excitation to select the optimal form of the arrays which serves our application.

With consideration given to the lightweight, easy integration and low radiation loss requirements that are essential in communication systems, novel array antennas based on substrate integrated waveguide (SIW) have been proposed and analyzed with several configurations.

III. Antennas Array Structure And Design

To improve the wide bandwidth and enhance the high gain, we extend the single element with a SIW circular sawtooth antenna with a circular slot for two SIW circular saw tooth antenna arrays for millimeter-wave application.

For reasons related to simulation assurance and result validation, two new arrays antenna 1x2 and 2x2 which operate on Ku / K bands application were simulated by two software HFFSS and CST MWS. The SIW antenna inserted in the substrate presented in this paper achieves improvements in the beamwidth. With an improvement in the simulated radiation efficiency, and the gains of 1x2, and 2x2 array antennas.

1x2 and 2x2 arrays antennas based on SIW with a SIW line feeding scheme having a phase delay characteristic and low radiation loss have been designed and investigated for a communication system. In the process of designing a four-element 2x2 microstrip patch array antenna, we will first look at the 1x2 sub-array with fed by microstrip line SIW with inset-fed on the patch.

A. 1x2 Elements Antenna Array

The geometry of the proposed 1x2 antenna sub-array based on SIW is illustrated in Fig.7.

The two-element sub-array and its feeding network are shown in Figure (7.a). The scattering coefficients were obtained by using HFSS software. Here, in Fig. 7, the patch elements are connected using a quarter wavelength impedance transformer method. The λ/4 transformer end connected to the taper, the taper and the junction circuit in the same figure are cascaded to form a microstrip power divider, a longer length is used in the wide pass band frequency. Then, the simulated design charts for optimum taper shapes are obtained.

A uniform array is defined by uniformly-spaced identical elements of equal magnitude with a linearly progressive phase from element to element. The array factor AF can be obtained by considering the individual elements as point (isotropic) sources. If the elements are of any other pattern, the total field pattern can be obtained by simply multiplying the AF by the normalized field pattern of the individual element [18].

$$AF = \sin\left(\frac{N}{2}\psi\right) \Big/ \sin\left(\frac{1}{2}\psi\right) \tag{6}$$

where :

$$\psi = kd_x \sin\theta + \beta$$

Equation (6) is the of a linear array located on the x-axis. The array consists of two point-to-point linked SIW cavities. For feeding the two cavities, as shown in Figure 2, a SIW sequential power divider is used. We first investigate the mode field of a circular SIW cavity.

To provide directive radiation performance, the antenna elements arranged with a separation distance less than λ (wavelength). A distance of (0.5 λ_0) between the antennas generates too much coupling (losses > 1 dB) for an intended application stated in [19]. In our work, a distance of (0.72 λ_0) is ideal because the couplings have significantly disappeared.

In our design procedure, the dimensions of the first geometry shown in Fig.7(a) are optimized using HFSS to obtain better response matching and high gain. The dimensions of the optimized parameters of the antenna array are

summarized in Table II. The problem with this type of excitation is that the quarter-wave line tends to radiate and therefore results to degrade the radiation pattern and the antenna performances. To validate the concept of the 1x2 antenna arrays above, we added the inset feed at the patch level.

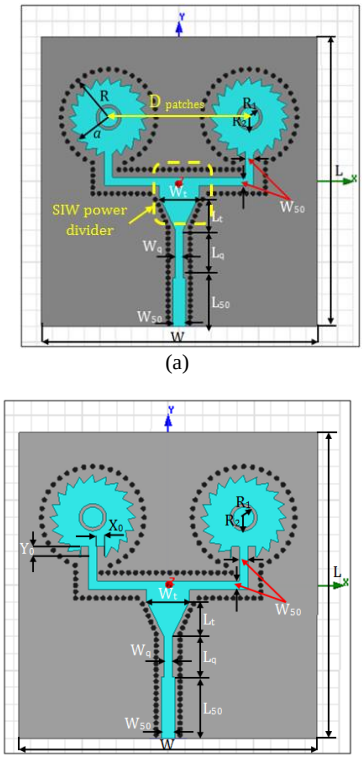

Fig.7. The geometry of the circular SIW 1x2 antenna array: (a) SIW μ-strip line feeding, (b) SIW inset feed line

The 50 Ω line excitation with inset feed consists to feed inside the patch of the second geometry shown in Fig. 7(b).The objective is to determine the optimal position on the patch so that the input impedance of the antenna is 50 Ω in order to be perfectly adapted.

TABLE II
ORIGINAL 1X2 ANTENNA ARRAY PARAMETERS

parameter	Description	Values (mm)
W	Width of the ground plane	11.6
L	length of the ground plane	12
P	Space between the via holes	0.8
a	The radius of the circular patch	4
L_{50}	length of the μ-strip fed line	7.2
W_{50}	width of the μ-strip fed line	1
L_q	length of μ-strip transformer fed line	4.8
W_q	width of μ-strip transformer fed line	1.6 W_{50}
W_t	width of the taper	5
R_1	The inner radius of the ring slot	1.2
R_2	The upper radius of the ring slot	1.6

To test the performance of the SIW inserted in the substrate, two sets of array antenna have been designed in a 1x2 array antenna based on SIW regarding the feeding type, feeding using SIW μ-strip feed line, and SIW Inset feed line. The simulations of the prototype responses prove that the circular SIW cavities inserted in the substrate provide lower losses and better performances.

Fig. 8 demonstrates the simulated reflection coefficient (S_{11}) of the two different feeding techniques. Minimum S_{11} is (-17 dB) approximately 12 GHz.

Acceptable S_{11} result of < -10dB is achieved for both 1x2 antenna array topologies with SIW feed line or with SIW inset feed line. However, with the SIW feed line, the simulated results show impedance bandwidths covering 140 MHz ranging from 11.99 to 12.13 GHz and 340 MHz from 18.89 to 19.23 GHz. Owing to the demand for a larger bandwidth is desired for satellite communications. Based on this initial sub-array, a modified design is further developed with an inset feed line that largely increases the simulated bandwidth of 170 MHz from 18.89 to 19.23 GHz and 410 MHz ranging from 20.36 to 20.77 GHz. The two resonances in the two *Ku* and *K* bands at the lower and the higher frequencies are due to the presence of the SIW cavity accompanied by the patch in the geometry of the arrays antenna, in which they are kept in convergent to achieve wide impedance bandwidth.

For this comparison, the second impedance bandwidth is more than the first.

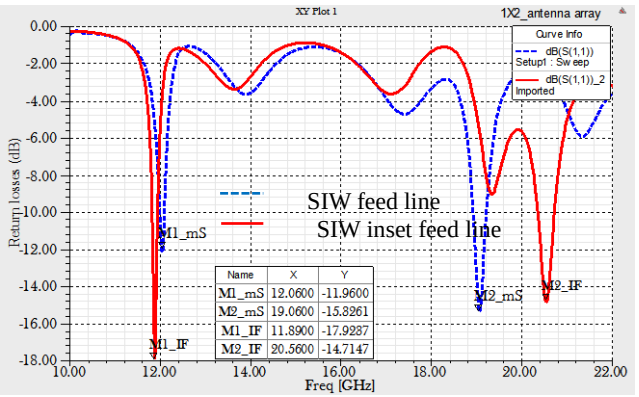

Fig. 8. Reflection coefficient of the two 1x2 antennas array based on SIW as the feeding of a) SIW feed line, b) SIW Inset feed line

In addition, since media decoder works with symbols from the same alphabet as used by the source, media decoder may entirely exploit the source redundancy to minimize error probability.

Figs. 9 (a) and (b), illustrate the plots of the simulated E plane and H-plane radiation patterns at the lower, and upper frequencies of both designs at which the maximum gain has occurred. The simulated radiation pattern of the 1x2 array antenna for the Ku/K band applications frequency allows visualization of the lobes in two dimensions, in the vertical plane ($\theta = 90$ °) including the largest lobe. By observing the radiation patterns, it can be seen that most of the radiation goes in the direction of the axis Oy.

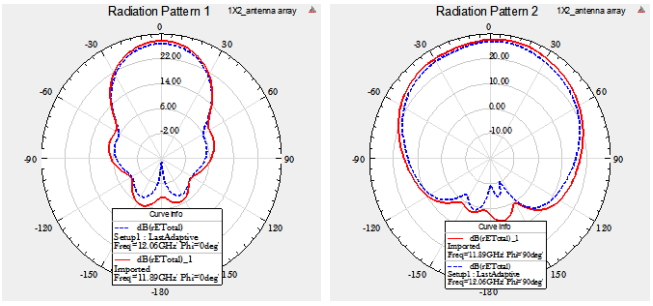

- E-Plane for φ=0° - H-Plane φ=90°

a. @ down frequencies of both topologies.

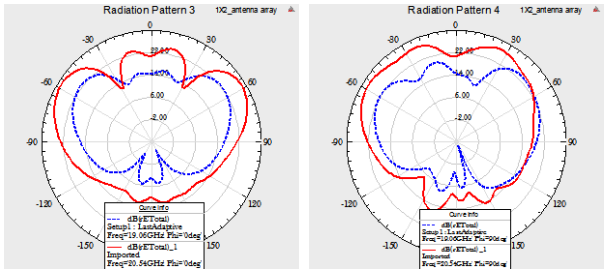

- E-Plane for φ=0° - H-Plane φ=90°

b. @ upper frequencies of both topologies.

Fig. 9. Simulated radiation patterns of1x2 antennas arrays

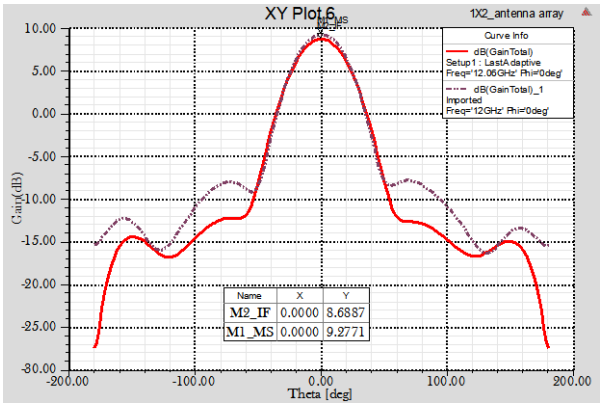

(a)

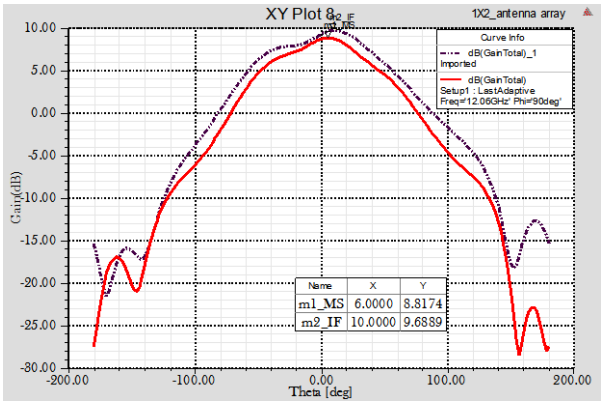

(b)

Fig.10. The simulated gain of (a) the 1x2 antenna array at 0 degrees of both designs, (b) the 1x2 antenna array at 90 degrees of both above designs

Fig. 10 shows the 2D plot of total gain versus theta for the 1x2 patch antenna array structures. The maximum total simulated gain is found to be 8.68dB array antenna - SIW μ-strip feed line and 9.27dB for the 1x2 array antenna - SIW inset feed line at 0 degrees whereas the maximum gain is 9.04 dB obtained for the 1x2 array antenna - SIW feed line and 9.68dB for the 1x2 array antenna - SIW inset feed line at 90 degrees. The electric field distributions are shown in Fig. 11.

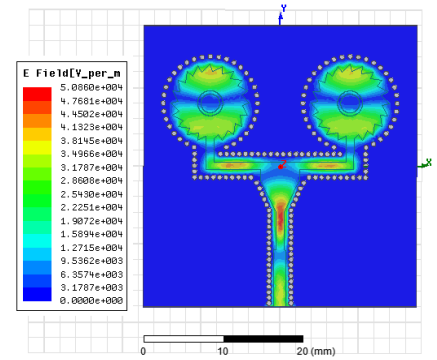

(a)

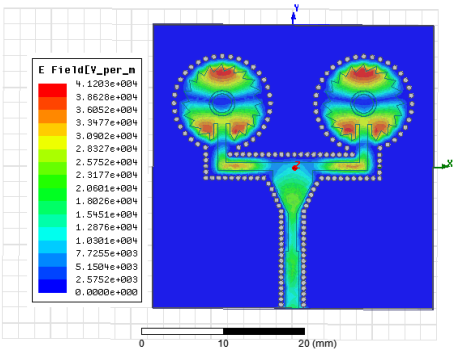

(b)

Fig. 11. Electric field distributions the 1x2 SIW antennas arrays(a) SIW feed line(b) SIW Inset feed line

The 1×2 sub-array presented in this section was studied in our previous work [10]. In [10], the proposed *array antenna* exhibited two bandwidths of 170 MHz and 410 MHz, a high gain of 9.27dB for the 1x2array antenna -SIW inset feed line. The comparison of the simulation results showed that the inset feed provides high bandwidth with the best matching. However, it is not sufficient for this we have increased the number of the patch in this work to conduct further improvements to the gain and bandwidth.

Therefore, we have designed a 2x2 antenna array as indicated in the following section. For the feeding, we chose the inset feed line because it is better matching than the microstrip line.

B. 2x2 Elements Antenna Array

Initially, a 1x2 antenna array is designed, optimized and characterized ranging from [11-21] GHz. After having the satisfying performance of the 1x2 SIW antenna array inset fed line a scale-down model is used to design the 2x2 SIW antenna array for Ku/K band application at dual-band. The design structure of the antenna array is shown in Fig.12.The

parametric study of the 1x2 SIW antenna array was repeated for the 2x2 array structure keeping the same cavity size.
The2x2 array antenna shown in Fig.12is composed of four SIW cavities to increase the total gain and improve the higher bandwidth.

A corporate feed network is designed to make the (2x2) array. Once the taper is designed, the next step is to design the junction branching from 25 Ω line to two 50 Ω lines. The design of a wideband 2-way microstrip power divider is demonstrated. The design mainly consists of two steps: the first is the design of taper that will provide wideband matching between the50 Ohms (Z_0)input line and 25 Ohms (Z_1) junction of output branches and the second is the design of the junction with very low return loss over a band wide as possible.

Then, a Klopfenstein Taper technique [20, 21] is employed, to transform the 100 ohms microstrip lines to 50 ohm lines, as:

$$\ln Z(z) = 0.5\ln(Z_0 Z_L) + \frac{c}{\cosh(A)}\Gamma_m A^2 \phi\left(\frac{2z}{L} - 1, A\right) \tag{7}$$

where:

$$A = \cosh^{-1}\left(\frac{\Gamma_m}{\Gamma_0}\right) \tag{8}$$

$$\Gamma_0 = \frac{1}{2}\ln\left(\frac{Z_L}{Z_0}\right) \tag{9}$$

$$\Gamma_m = \frac{\Gamma_0}{\cosh(A)} \tag{10}$$

where:
c: is the speed of light.
L: is the taper length,
B: is the propagation constant
Γ_m: is the minimum reflection coefficient.
Γ_0: is the reflection coefficient at zero frequency.
Z_0 and Z_L are the characteristic impedance at the ends of the taper and the function ϕ (z,A) is defined as:

$$\phi(z, A) = \int_0^X \frac{I_1(A\sqrt{1-y^2})}{(A\sqrt{1-y^2})} dy \qquad For|z|\langle 1 \tag{11}$$

where I_1 is the modified Bessel function.
The reflection coefficient is given by:

$$\Gamma = \Gamma_0 e^{-j\beta z}\frac{\cos\sqrt{(\beta L)^2 - A^2}}{\cosh(A)} \qquad For \beta L \rangle A \tag{12}$$

$$\Gamma = \Gamma_0 e^{-j\beta z}\frac{\cos\sqrt{A^2 - (\beta L)^2}}{\cosh(A)} \qquad For \beta L \langle A \tag{13}$$

After the tapered design is completed, the junction with 12.5 Ω line input and two 25 Ω is designed with a minimum reflection coefficient having a frequency band wide as possible. Then, the junction of a 25 Ω input and two 50 Ω output such as in Fig. 12 is added on each side. The final circuit is formed with the inclusion of optimally designed mitered bends. The designed circuit is displayed in Fig. 12.

Apart from the feed technique, another parameter that plays a very important role in achieving the performance of an antenna array is the spacing between the network elements.

The elements are arranged uniformly along a rectangular grid in the *xy*-plane, with an element spacing *dx* in the *x*-direction and an element spacing d_y in the *y*-direction to reduce mutual coupling between the elements.

Several investigators have considered the patch as a cavity that acts as a disc resonator. In such a geometry TM_{nm} mode with respect to y-axis are excited. The subscripts *n* and *m* are the mode numbers associated with *x* and y-directions respectively.

The total fields of the present array antenna can be expressed by the fields of a single clement positioned at the origin, multiplied by the array factor. This method is widely known as a pattern multiplication approach[22]. Since the entire array is taken as uniform, the normalized form of array factor (AF) is obtained and may be written as**:**

$$AF(\theta,\phi) = \left[\frac{1}{M}\frac{\sin(\frac{M}{2}(kd_x \sin\theta\cos\phi + \beta_x))}{\sin(\frac{1}{2}(kd_x \sin\theta\cos\phi + \beta_x))}\right] \left[\frac{1}{N}\frac{\sin(\frac{N}{2}(kd_y \sin\theta\sin\phi + \beta_y))}{\sin(\frac{1}{2}(kd_y \sin\theta\sin\phi + \beta_y))}\right] \tag{14}$$

where
k: Phase propagation constant for EM wave.
β_x, β_y: Progressives phase excitation of difference along *x* and *y* directions, respectively.
d_x, d_y: Separation between the elements along *x* and *y* directions, respectively.

3D view

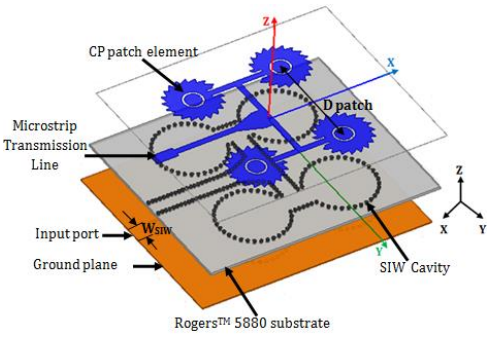

Side view

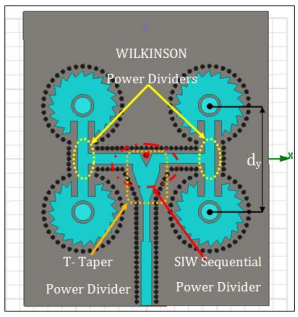

Fig.12. Configuration of the original 2 × 2 antenna array. (Top):3Dview with different layers; and (Bottom): Side view of power dividers and phases delay

In our case, the inter-element spacing's are chosen to be $d_x=0.72\lambda$ *and* $d_y=0.64\lambda$ *and* $M=N=2$, to obtain the optimum gain, satisfying bandwidth and, reduce mutual coupling between the elements. The design and simulation of the structure are performed on the Ensemble platform. After achieving optimum input impedance, return losses (RL), isolation, radiation patterns, and gain, a prototype model is validated with the CST MWS.

IV. Results And Discussion

The simulated input impedance of the feeding 2x2 array antenna is plotted in Fig. 13; these simulation results state a good adaptation for our antenna array at the resonance frequencies. The 2D parallel SIW Inset feed line array was composed of power dividers and impedance transformers with two impedances of 52 Ω at 13.18GHz, and 60Ω at 21.54 GHz.

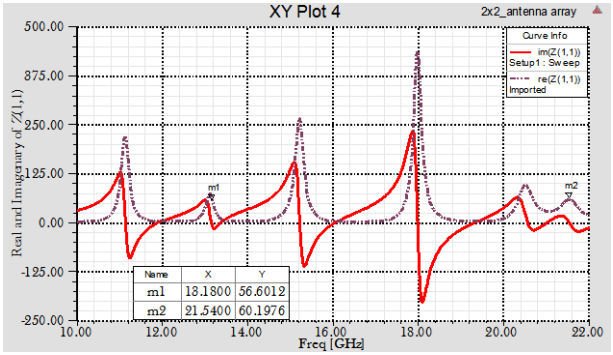

Fig.13. Real and imagined input impedance of 2x2 sub-array antenna

Fig. 14 illustrates the simulated performance of the 2x2 sub-arrays with the SIW inset feed line. The antenna bandwidth is found to be 210 MHz (12.97–13.39) GHz for first operating bandwidth at the Ku-band while the second located at K-band having a bandwidth found to be approximately 1.31 GHz (20.23–22.72) GHz. The simulated peak gain and the realized gain are found to be 9.05 dB and 37.8dB respectively at the center frequency, which is more than two times wider than the operating bandwidths of the initial designs.

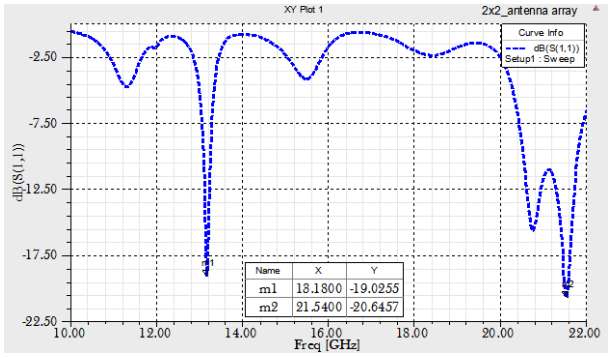

(a)

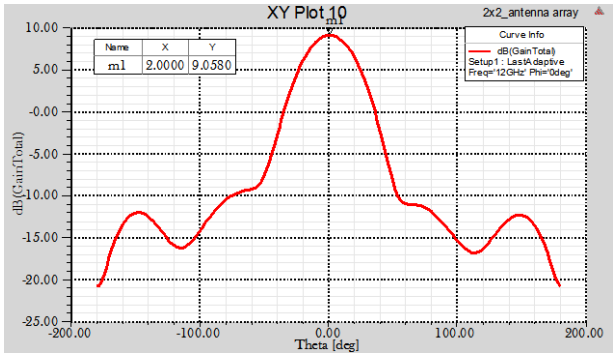

(b)

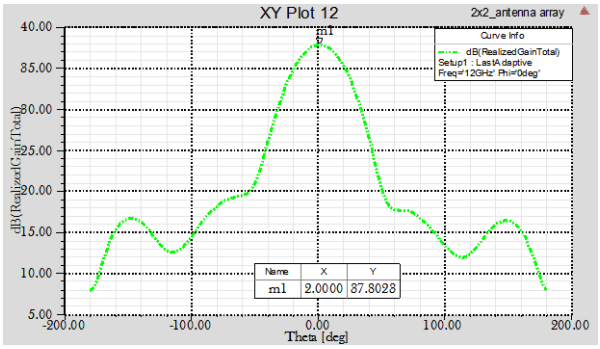

(c)

Fig.14. Simulated results of theCP2x2 SIW sub-array antenna. (a) S_{11}, (b) Gain at, and (c) Realized peak gain

The radiation pattern of the array antenna in the E plane (horizontal plane) and the H plane (vertical plane) remains good over the entire frequency band used. The comparison of two-dimensional (2D) radiation patterns obtained from HFSS at lower and upper resonance frequencies in the vertical (φ= 90°) and horizontal (φ= 0°) planes is illustrated in Fig. 15 (from "a" to "d") respectively. Finally, the distribution of the electric field in the array antenna is illustrated in Fig. 16.

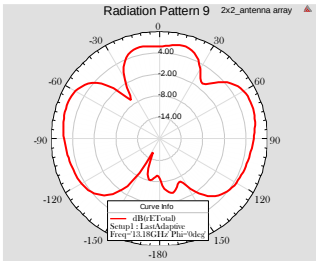

(a) E-Plane at 13.18 GHz

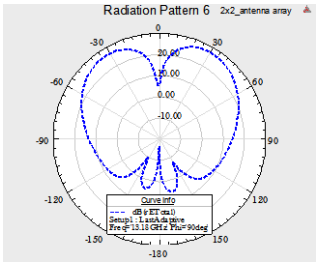

(b) H-Plane at 13.18 GHz

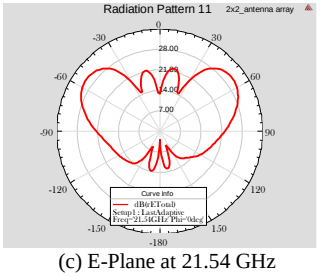

(c) E-Plane at 21.54 GHz

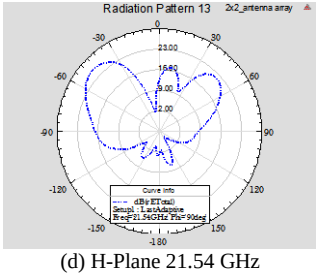

(d) H-Plane 21.54 GHz

Fig. 15. Simulated radiation patterns of the 2x2 SIW antenna array

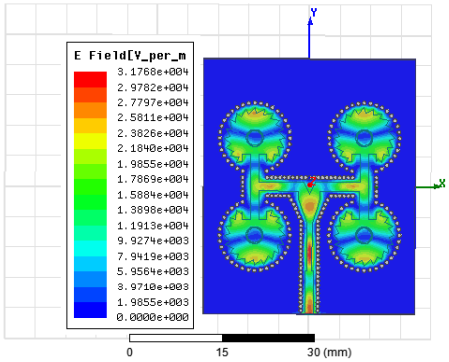

Fig. 16. The simulated electric field of the 2x2 SIW antenna array

Table III illustrates the electrical performances of the three proposed SIW structures antennas. As expected, the increase in antenna elements accompanied by SIW sequential power divider results in higher gain and wider bandwidth. To sum up, Table III conducts a comparison in terms of the main characteristics related to our designs and other reported works. It is can be noticed that our design achieves the highest gain and fulfilling bandwidth.

TABLE III
SUMMARIZES GAIN AND BANDWIDTH FOR THE ANTENNA CONFIGURATIONS SIMULATED

	Gain (dB)	Resonances frequency (GHz)		S_{11}(dB)		Bandwidth (MHz)	
		f_D	f_U	$(S_{11})_D$	$(S_{11})_U$	BW_D	BW_U
Prototype-single element	4.83	11.77	19.97	-15.77	-33.32	250	470
1x2 elements With SIW feed line	8.68	12.06	19.06	-12.44	-14.63	140	340
1x2 elements With SIW inset feed line	9.27	11.89	20.56	-17.92	-14.71	170	410
2x2 elements array	9.05	13.18	21.54	-19.02	-20.64	210	1310

Table IV compares various characteristics between our designs and those of other references. We conclude that our designs have a low weight, the highest gain, and acceptable bandwidth. It is considered a superior candidate for Ku/K band applications.

Some key milestones to conclude our work, it was designed then passed through other simulations software associated with reflection or radiation. This validation is carried out by CST MWS. Two versions of the (1x2) and (2x2) array antennas were designed and tested using electromagnetic software: Ansoft HFSS based on the Finite Element Method (FEM) and CST Microwave Studio based on the Finite Integration Technique (FIT).

TABLE IV
COMPARISON BETWEEN OUR DESIGN AND OTHER REFERENCES

Ref.	Radiating elements	Realized Gain (dB)	Bandwidth (GHz)
[23]	4 × 4	14	8
[24]	4 × 4	19.5	-
[25]	8 × 8	26.1	8.85
[26]	4 × 4	18.2	9.5
[27]	4 × 4	18.7	2.75
[28]	4 × 4	15.8	-
[29]	2 × 2	12.5	-
[30]	16 x 6	26.4	0.85
Our design	2 × 2	37.8	1.31

Therefore, we propose a comparative study between the SIW sawtooth antenna and the 1 x2 linear antenna arrays and the 2x2 planar arrays for the [10-22 GHz] frequency range. This comparison includes the results obtained by ANSYS HFSS and their validation with CST MWS is illustrated in the figures down below.

Figs. 17 and 18 illustrate the simulated results of the SIW1x2sub-array antennas with inset feed and the 2x2 SIW antenna array in terms of reflection coefficient and E-field distribution respectively, which were obtained from HFSS software and CST MWS.

In Fig. 17, the reflection coefficient S_{11} obtained from CST and HFSS shows that there is a good agreement between the simulated return losses obtained using two software.

A slight difference in the two simulated is essentially due to the two different numerical methods employed by the ANSYS HFSS and the CST Microwave Studio. Regarding peak gain, a better agreement between the results can be observed in Fig. 18.

This comparison shows that we got the goal. It can be noticed that the feeding circuit works perfectly in our array antennas. A representation of the three-dimensional diagram is shown in Fig. 18 for the three configurations performed.

The maximum radiation is in the plane of alignment of the grating (plane $\theta = 90$ °), maximum of directivity and, gain. The opening of the main lobe of a network with a small number of radiating elements is wider than that of a network with a high number of elements; also, the number of side lobes increases according to the number of radiating elements in the network.

From the results, we can conclude that the more the number of radiating elements increases the more the main lobe becomes very narrow and amplified the directional gain and the total gain in a definite direction.

However, we can reasonably estimate that a gain of a few dB in the gain level can be realized, which is also related to the adaptation solutions. It should approach the level of directivity which is in the order of 11dB. The objective is therefore attainted.

The peak gain values are stated for both of HFSS and CST MWS results in table V. The table confirms the good agreement between the results of the two software.

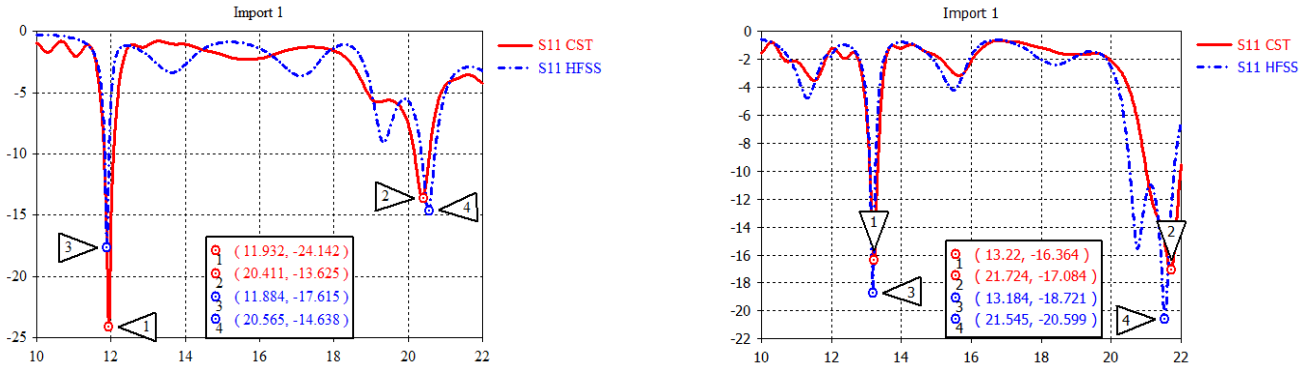

(a) (b)

Fig. 17. The coefficient S_{11} obtained from CST and HFSS (a) of 1x2 SIW sub-array antennas with inset feed and (b) 2x2 SIW antenna.

Results of 1x2 SIW saw tooth antenna sub-array from HFSS *Results of 1x2 SIW saw tooth antenna sub-array from CST*

Gain E-Plane Gain E-Plane

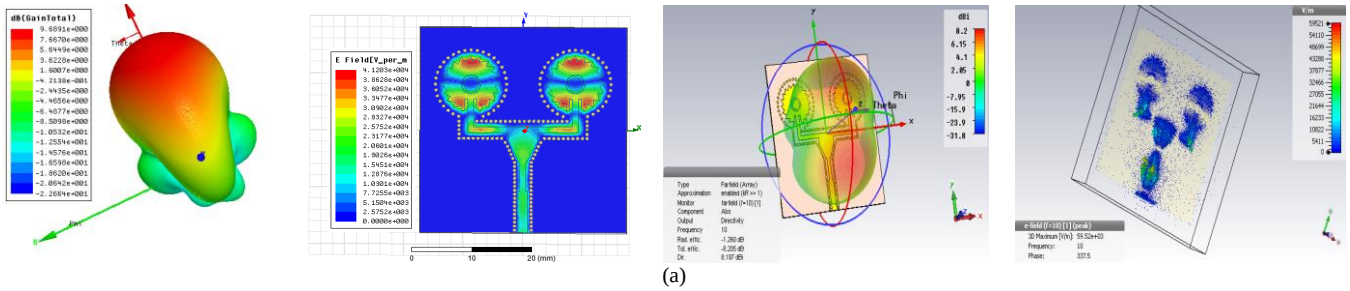

(a)

Results of 2x2 SIW saw tooth antenna sub-array from HFSS *Results of 2x2 SIW saw tooth antenna sub-array from CST*

Gain E-Plane Gain E-Plane

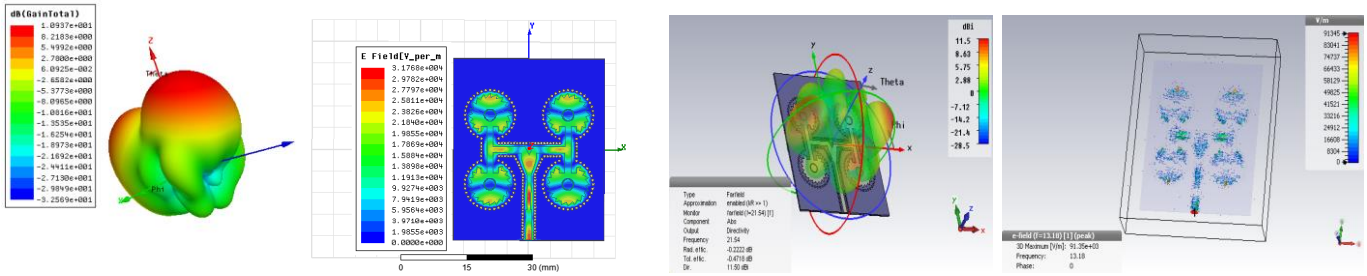

(b)

Fig. 18. Electrical parameters of the SIW saw tooth antenna for both designs (gains and electric fields) from HFSS and CST (a) of 1x2 SIW sub-array antennas with inset feed and (b) 2x2 SIW antenna

TABLE V
THE CST AND HFSS SIMULATED PEAK GAIN AND BANDWIDTH OF THE PROPOSED ANTENNA

Antenna array	Simulator	@ *Ku* band			@ *K* band			3DPeak gain (*dB*)
		f_D (*GHz*)	S_{11}(*dB*)	*BW*(*MHz*)	f_U(*GHz*)	S_{11}(*dB*)	*BW*(*MHz*)	
1x2	HFSS	11.89	-17.92	170	20.54	-14.82	410	9.68
	CST	11.93	-23.8	260	20.40	-13.65	410	8.2
2x2	HFSS	13.18	-19.02	210	21.54	-20.64	1310	10.93
	CST	13.22	-16.36	220	21.72	-17.10	1020	11.5

V. Concluding Remarks

In this paper, a new single antenna and array antennas based on SIW- have been suggested, studied, designed and discussed in terms of electrical performances. The first array consists of two elements with two SIW circular cavities fed using SIW power divider. The second array consists of two elements with two SIW circular cavities which fed by a SIW inset fed line. The simulation results of these two types of arrays show that the second structure presents better performances than the first one. We expanded this structure into a 4-elements (2 × 2) array with a compact rotation feeding technique to expand the operating bandwidth and obtain a higher gain twice the original design. Simulated results of this structure show excellent radiation performance in terms of bandwidth, realized gain and, radiation pattern. The planar antenna array is a good candidate for communication systems preferring high gain, in particular, *Ku/K* band applications. The HFSS is used for simulation and investigation of the designed 1x2 SIW sub-array sawtooth antenna feeding by inset feed line and the 2x2 antenna array, the results obtained were confirmed by the comparison of these results with those obtained by CST MWS simulation tool.

References

[1] Alhalabi, R.A.; Rebeiz, G.M. "High-gain yagi-uda antennas for millimeter-wave switched-beam systems". IEEE Trans. Antennas Propag., 57, 3672–3676, DOI:10.1109/TAP.2009.2026666.2009.

[2] Yu Jian Cheng, "Substrate Integrated Antennas and Arrays", Taylor& Francis Group, LLC CRC Press is an imprint of Taylor & Francis Group, an Informa business, 2016.

[3] Syrytsin, I.; Zhang, S.; Pedersen, G.F.; Ieee, S.M.; Morris, "A compact Quad-Mode Planar Phased Array with Wideband for 5G Mobile Terminals". IEEE Trans. Antennas Propag. DOI 10.1109/TAP.2018.2842303. 2018.

[4] Mikulasek, T., Georgiadis, A., Collado, A., &Lacik. "2x2 Microstrip Patch Antenna Array Fed by Substrate Integrated Waveguide for Radar Applications". *IEEE Antennas and Wireless Propagation Letters, 12*, 1287-1290, DOI: 10.1109/LAWP.2013.2283731.J. 2013.

[5] Bozzi, M., Pasian, M., Perregrini, L., K.Wu, "On the losses in substrate integrated waveguides". In Proceedings of the European Microwave Conference, p. 384–387, DOI: 10.1109/EUMC.2007.4405207. 2007.

[6] W. M. Abdel-Wahab and S. Safavi-Naeini, "Wide-bandwidth 60-GHz aperture-coupled microstrip patch antennas (MPAs) fed by substrate integrated waveguide (SIW)," IEEE Antennas Wireless Propag. Lett. vol. 10, pp. 1003-1005, DOI:10.1109/LAWP.2011.2168373. 2011.

[7] Nouri Keltouma, Feham Mohammed and Adnan Saghir," Design and characterization of tapered transition and inductive window filter based on Substrate Integrated Waveguide technology (SIW)", IJCSI International Journal of Computer Science Issues, Vol. 8, Issue 6, No 3, November 2011.

[8] Damou Mehdi, Nouri Keltouma and Feham Mohammed, "Design for Tapered transitions From Microstrip Lines to Substrat Integrated Waveguide at Ka-Band", IJCSI International Journal of Computer Science Issues, Volume 12, Issue 2, March 2015.

[9] Keltouma Nouri, Tayeb Habib Chawki Bouazza, Boubakar Seddik Bouazza, Mehdi Damou, Kada Becharef, and SalimaSeghier "Design of Substrate Integrated Waveguide Multi-band Slots Array Antennas" International Journal of Information and Electronics Engineering Vol. 6, No. 4, DOI: 10.18178/ijiee.2016.6.4.628. July 2016.

[10] ABES Turkiya; NOURI Keltouma; BOUAZZA Boubakar Seddik; BECHAREF Kada and Damou Mehdi, '' Gain Enhancement of Microstrip Sawtooth Antenna Array based on Substrate-Integrated Waveguide Technology for Dual-Band Applications (Ku / K)'', the IEEE sixth international conference on the image and signal processing and their applications(ISPA), Mostaganem, Algeria. DOI: 10.1109/ISPA48434.2019.8966817. Nov2019.

[11] F. Xu and K.Wu, "Guided-wave and leakage characteristics of substrate integrated waveguide," IEEE Trans. Microw. Theory Tech, vol. 53, no. 1, pp. 66–73, DOI: 10.1109/TMTT.2004.839303. Jan. 2005.

[12] F. Xu, Y. L. Zhang, W. Hong, K. Wu, and T. J. Cui, "Finite-difference frequency-domain algorithm for modeling guided-wave properties of substrate integrated waveguide," IEEE Transactions on Microwave Theory and Techniques, vol. 51, pp. 2221-2227, DOI: 10.1109/TMTT.2003.818935. Nov 2003.

[13] H. Uchimura, T. Takenoshita, and M. Fujii, " Development of a laminated waveguide", IEEE Transactions on Microwave Theory and Techniques, vol. 46, pp. 2438-2443, DOI: 10.1109/22.739232. Dec 1998

[14] D. Deslandes and K. Wu, "Substrate integrated waveguide leaky-wave antenna: Concept and design considerations," presented at the Asia–Pacific Microw. Conf. (APMC), Sochou, China, https://doi.org/10.1155/2015/359670. Dec. 2005

[15] Zhen Tu, Dong-Fang Zhou, Guang-Qiu Zhang, Feng Xing, XueLeiand De-Wei Zhang," A wideband cavity-backed elliptical printed dipole antenna with enhanced radiation patterns," IEEE Antennas and wireless propagation. vol. 12, pp. 1610-1613. DOI: 10.1109/LAWP.2013.2294058. 2013

[16] Sumin Yun, Dong-Yeon Kim, and Sangwook Nam," Bandwidth enhancement of cavity-backed slot antenna using a via-hole above slot". IEEE Antennas and wireless propagation. vol. 11, pp. 1092-1095. DOI:10.1109/LAWP.2012.2215911. 2012.

[17] M. Sharifian Mazraeh Mollaei, and S. H. Sedighy "Three bands Substrate Integrated Waveguide Cavity Spatial Filter with Different Polarization" IEEE Transactions on Antennas and Propagation: DOI 10.1109/tap.2017.2736527, 0018-926x (c) .2017.

[18] J.C. Iriarte, I. Ederra, R. Gonzalo and P.de Maagt. "Coupling reduction in a 2x2 high dielectric constant ebg patch array". In Antenna Technology (iWAT), International Workshop on, pages 1–2, March 2010.

[19] T. C. Cheston, *and* J. Frank, *"*Phased Array Radar Antenna*"*, McGraw Hill, *Edition New York*, 1990

[20] Deshmukh A.A, Ray K.P, Chine P.N. ''Multi-band stub loaded Square ring Microstrip antennas'', Applied Electromagnetics Conference'' (AEMC), P. 1−4. DOI:10.1109/AEMC.2009.5430706. Dec 2009.

[21] Esa M, Malik N.N.N.A, Latif N.A, Marimuthu J. "performance investigation of Microstrip exponential tapered line impedance transformer using math CAD", Progress in Electromagnetics Research Symposium Proceedings.; p. 1209−13.P Mid: 19786392. Aug 2009

[22] D. Kajfez and J. Prewitt, "Correction to a transmission line taper of improved design," IEEE Transactions on Microwave Theory and Techniques, vol. MTT-21, p. 364, DOI: 10.1109/TMTT.1973.1128003. May 1973.

[23] W. Lin and H. Wong, "Multi-polarization reconfigurable circular patch antenna with L-shaped probes," IEEE Antenna and Wireless Propag. Letters, vol.16, pp. 154 9-1552, DOI 10.1109/LAWP.2017.2648862. 2017.

[24] C Liu, Y. X. Guo, X. Bao and S. Q. Xiao, "60-GHz LTCC integrated circularly polarized helical antenna array," IEEE Trans. Antennas Propag., vol. 60, no. 3, pp. 1329–1335, DOI: 10.1109/TAP.2011.2180351. Mar. 2012.

[25] Q. Zhu, K. B. Ng and C. H. Chan, "Printed Circularly Polarized Spiral Antenna Array for Millimeter-Wave Applications," IEEE Trans. Antennas Propag., vol. 65, no. 2, pp. 636–643, DOI: 10.1109/TAP.2016.2640019 Feb. 2017

[26] H. Sun, Y. X. Guo and Z. Wang, "60-GHz circularly polarized U Slot patch antenna array on LTCC," IEEE Trans. Antennas Propag., vol. 61, no. 1, pp. 430–435, DOI: 10.1109/TAP.2013.2280873. Jan. 2013.

[27] D. F. Guan, C. Ding, Z. P. Qian, Y. S. Zhang, Y. J. Guo and K. Gong "Broadband high-gain SIW cavity-backed circular-polarized array antenna," IEEE Trans. Antennas Propag., vol. 64, no. 4, pp. 1493–1497, DOI: 10.1109/TAP.2016.2521904. Apr. 2016.

[28] J. Wu, Y. J. Cheng and Y. Fan, "Millimeter-wave wideband high efficiency circularly polarized planar array antenna," IEEE Trans. Antennas Propag., vol. 64, no. 2, pp. 535–542, DOI: 10.1109/TAP.2015.2506726. Feb. 2016.

[29] Y. Li and K. M. Luk, "A 60-GHz Wideband circularly polarized aperture-coupled magneto-electric dipole antenna array," IEEE Trans. Antennas Propag, vol. 64, no. 4, pp. 1325–1333, DOI: 10.1109/TAP.2016.2537390. Apr. 2016.

[30] J.Q. Huang, W. Lin, "A Low Profile, Ultra-Lightweight, High Efficient Circularly-Polarized Antenna Array for Ku Band Satellite Applications". DOI:10.1109/ACCESS.2017.2750318, IEEE Access· September2017.

Turkiya Abes was born in Saida, Algeria. She is a PhD student at the Faculty of Technology, Dr. Moulay Tahar Saida, Algeria. Her research interests include microwave planar, SIW technologies which are antennas and metamaterials compenents.

Keltouma Nouri was born in Saida, Algeria. Her degree of bachelor in communication engineering was earned from Abou Bekr Belkaid in Telmcen, Algeria. She is now an professor in Dr. Moulay Tahar University, Saida, Algeria. Her research interests are mainly in microwave planar and SIW technologies, which are filters, couplers, attenuators, antennas and metamaterials components.

Boubaker Seddik Bouazza was born in Algeria. He is professor. His research work is mainly focused on channel coding for communication systems and metamaterials components.

Kada Becharef was born in Algeria, PhD in Communication Technology, Dr. Moulay Tahar Saida, Algeria. His research interests include metamaterials components: filters, couplers, dividers.